Carbon nanotube Bloch equations: A many-body approach to nonlinear and ultrafast optical properties

Matthias Hirtschulz,[1,*] Frank Milde,[1] Ermin Malić,[1] Stefan Butscher,[1] Christian Thomsen,[2] Stephanie Reich,[3] and Andreas Knorr[1]

[1]*Institut für Theoretische Physik, Technische Universität Berlin, 10623 Berlin, Germany*

[2]*Institut für Festkörperphysik, Technische Universität Berlin, 10623 Berlin, Germany*

[3]*Fachbereich Physik, Freie Universität Berlin, 14195 Berlin, Germany*

(Received 19 September 2007; published 3 January 2008)

Carbon nanotube Bloch equations are proposed to analyze the many-body electron dynamics for optical interband transitions in carbon nanotubes. As a first approach, the Bloch equations for microscopic transitions and occupations are discussed within the screened Hartree-Fock approximation. The potential of the Bloch equation approach is illustrated for linear and nonlinear optical spectra and ultrafast electron dynamics in carbon nanotubes.

DOI: 10.1103/PhysRevB.77.035403 PACS number(s): 78.67.Ch, 73.22.−f, 42.65.−k

INTRODUCTION

The electronic and optical properties of carbon nanotubes (CNTs) are dominated by many-body effects, such as electron-electron and electron-phonon interactions. Examples include the formation of excitons[1,2] and their coupling to vibronic modes.[3] Recent theoretical work on CNTs is focused on the stationary response of these nanotube excitations to cw fields: Several frequency range descriptions, using Hubbard models[4,5] or *ab initio* approaches based on density functional theory methods and the Bethe-Salpeter equation,[6,8,7] have been developed.

In this paper, we describe a *dynamical approach* to CNT properties which can be used to directly describe their linear and nonlinear optical response to ultrashort optical pulses. For this purpose, the many-body density matrix theory[9–12] is combined with tight-binding band structure calculations of CNTs.[13,14] We show that the derived carbon nanotube Bloch equations (CNBEs) contain excitons as elementary optical excitations, both for weak excitation as well as for optical nonlinearities, including gain for high excitation. We illustrate the temporal response to ultrashort pulses by calculating the time dependence of the electron density and the optical Stark effect. Our goal is to give compact equations for the CNT interband optical transitions and band occupations that can be used to describe experiments relying on testing temporally resolved quantities.[15,16]

Our starting point is the CNT Hamiltonian $H=H_f+H_{ee}$, where $H_f=H_0+H_{A\text{-}el}$ is the free particle electron Hamiltonian in the tight-binding approximation containing the single-particle energy and the electron-light interaction for a spatially homogeneous field (long wavelength approximation). Here, H_{ee} accounts for the electron-electron interaction. The theory is evaluated in second quantization to include the fermionic character of the CNT electrons,

$$H_f = \sum_1 E(1) a_1^\dagger a_1 - \frac{e_0 \hbar}{i m_0} \mathbf{A}_t \cdot \sum_{1,2} \mathbf{M}_{12} a_1^\dagger a_2, \tag{1}$$

$$H_{ee} = \frac{1}{2} \sum_{1,2,3,4} V_{\substack{12\\34}} a_1^\dagger a_2^\dagger a_4 a_3. \tag{2}$$

Here, $a_1^\dagger$ (a_1) creates (destroys) an electron with the compound quantum number $1=(\lambda_1,\mathbf{k}_1)$, describing CNT states in band λ_1 including the electronic wave number $\mathbf{k}_1=\mathbf{k}_{1\parallel}+\mathbf{k}_{1\perp}$. Moreover, $\mathbf{k}_{1\parallel}$ is the continuous component parallel to the nanotubes axis, while $\mathbf{k}_{1\perp}$ is the discrete, perpendicular component in the zone-folding approximation. $E(1)=E_{\lambda_1}(\mathbf{k}_1)$ are the tight-binding single-particle energies.[13] $\mathbf{A}_t$ is the time dependent vector potential describing an incident optical pulse. $\mathbf{A}_t$ is split into a fast rotating term with frequency ω_L and a slowly varying pulse envelope $\mathbf{A}_0(t)$: $\mathbf{A}_t=\mathbf{A}_0(t)(e^{i\omega_L t}+e^{-i\omega_L t})$. The single-particle tight-binding wave functions $|\lambda,\mathbf{k}\rangle$ have the form[13]

$$\Psi_\lambda(\mathbf{k},\mathbf{r}) = \frac{1}{\sqrt{N}} \sum_{s=A,B} \sum_j C_s(\lambda,\mathbf{k}) e^{i\mathbf{k}\cdot\mathbf{R}_j^s} \varphi(\mathbf{r}-\mathbf{R}_j^s), \tag{3}$$

with N the number of graphene unit cells in the single-walled carbon nanotube. Here, $\varphi(\mathbf{r}-\mathbf{R}_j^s)$ are the $2p_z$ atomic orbitals located at the lattice positions $\mathbf{R}_j^s$, where s labels the two sublattices and j the atomic positions. $\mathbf{M}_{12}=\delta_{\mathbf{k}_1,\mathbf{k}_2}\langle 1|\nabla|2\rangle$ are the optical momentum matrix elements in a tight-binding basis analyzed in detail in Refs. 17–19. m_0 denotes the free electron mass and e_0 the elementary charge. $V_{\substack{12\\34}}=\langle 1|\langle 2|V(\mathbf{r}-\mathbf{r}')|3\rangle|4\rangle$ are the Coulomb matrix elements[20] and $V(\mathbf{r}-\mathbf{r}')$ is the Coulomb potential. As the bare Coulomb potential can give rise to infinite exciton binding energies in one-dimensional systems, a regularized CNT Coulomb potential is used to account for the finite tube radii. This is done by averaging the three-dimensional Coulomb potential using an electron density $\frac{1}{2\pi\rho_0}\delta(\rho-\rho_0)$ (ρ_0 is the radius of the CNT). This procedure leads to Coulomb matrix elements similar to Ref. 21, but it also takes into account the properties of the tight-binding wave functions and atomic orbitals,

$$V^{\boldsymbol{\lambda}}_{\substack{\mathbf{k}+\mathbf{q},\mathbf{k}\\ \mathbf{k},\mathbf{k}+\mathbf{q}}} = V^{\boldsymbol{\lambda}}_{(\mathbf{k},\mathbf{q})} = \frac{\alpha_{\boldsymbol{\lambda}}(\mathbf{k},\mathbf{q})}{\varepsilon_r \varepsilon(q_\parallel) S(q_\parallel)} I_0(|q_\parallel|\rho_0) K_0(|q_\parallel|\rho_0). \quad (4)$$

Here, $\alpha_{\boldsymbol{\lambda}}(\mathbf{k},\mathbf{q})$ is a factor accounting for the CNT structure via the tight-binding wave functions with the band index $\boldsymbol{\lambda}=(\lambda_1,\lambda_2,\lambda_3,\lambda_4)$, $S(q_\parallel)=(P_0^2+q_\parallel^2)^6$, $I_0(x)$ (K_0) are the modified Bessel function of the first (second) kind, $\varepsilon(q_\parallel)$ is the internal static $(\omega\to 0)$ screening in random phase approximation,[20] ε_r is the background dielectric (external) screening constant ($\varepsilon_r=1$ throughout this paper), and $P_0=Z_{eff}/a_B$, where Z_{eff} is an effective atomic number and a_B is the Bohr radius.

To illustrate the potential of our approach, we focus on one valence ($\lambda=v$) and one conduction ($\lambda=c$) band (p_z orbitals) and include only the two subbands at the minimum gap energy. Further subbands or valence and conduction bands (σ orbitals) can be included in a similar fashion. For a spatially homogeneous carrier distribution along the CNT, the expectation values of two operators $p_{\mathbf{k}}(t):=\langle a^\dagger_{v\mathbf{k}} a_{c\mathbf{k}}\rangle$ and $n^\lambda_{\mathbf{k}}(t):=\langle a^\dagger_{\lambda\mathbf{k}} a_{\lambda\mathbf{k}}\rangle$ describe the transition probability amplitudes between the two bands and the occupations of band λ ($\lambda=c,v$) at wave number $\mathbf{k}$, respectively. These quantities can be used to calculate the total electron $n^\lambda(t)$ and current density $\mathbf{j}(t)$ as a function of time,[20]

$$n^\lambda(t) = \frac{2e_0}{L_\parallel}\sum_{\mathbf{k}} n^\lambda_{\mathbf{k}}(t),$$

$$\mathbf{j}(t) \sim \sum_{\mathbf{k}} [\mathbf{M}^{vc}_{\mathbf{k}} p_{\mathbf{k}}(t) + \text{c.c.}], \quad (5)$$

with $L_\parallel$ the length of the nanotube. $n^\lambda(t)$ and $\mathbf{j}(t)$ as macroscopic quantities can be used to characterize the absorption spectra or the ultrafast response, both accessible in experiments. $n^\lambda(t)$ and $\mathbf{j}(t)$ will be calculated via a Bloch equation approach for CNTs.

CARBON NANOTUBE BLOCH EQUATIONS

To obtain the current and charge density [Eq. (5)], the equations of motion (EOMs) for the microscopic transition amplitudes $p_{\mathbf{k}}(t)$ and occupations $n^\lambda_{\mathbf{k}}(t)$ are derived from the Heisenberg equation of motion $i\hbar\dot{O}=[O,H]$ for an observable O. Evaluating the commutator, we find the free carrier propagation and the electron-field and the electron-electron contributions, $\dot{p}_{\mathbf{k}}=\dot{p}_{\mathbf{k}}|^0+\dot{p}_{\mathbf{k}}|^{A\text{-}el}+\dot{p}_{\mathbf{k}}|^{ee}$ [analog equation for $n^\lambda_{\mathbf{k}}(t)$]. Employing the rotating wave approximation (RWA) with the ansatz $p_{\mathbf{k}}(t)\to p_{\mathbf{k}}(t)e^{-i\omega_L t}$, we find for $p_{\mathbf{k}}(t)$,

$$\dot{p}_{\mathbf{k}}|^0 + \dot{p}_{\mathbf{k}}|^{A\text{-}el} = i(\omega_L - \omega^{cv}_{\mathbf{k}})p_{\mathbf{k}} - \Omega(n^v_{\mathbf{k}} - n^c_{\mathbf{k}}), \quad (6)$$

where $\Omega=\frac{e_0}{m}\mathbf{A}_0(t)\cdot\mathbf{M}^{vc}_{\mathbf{k}}$. The energy dispersion of the interband transition $\omega^{cv}_{\mathbf{k}}=[E_c(\mathbf{k})-E_v(\mathbf{k})]/\hbar$ is calculated from the tight-binding band structure.[14] The Pauli blocking (second term), which reduces the electron-light coupling if $n^c_{\mathbf{k}}(t)\neq 0$ (finite conduction band electron density), is determined by the difference of the band occupations $n^v_{\mathbf{k}}(t)-n^c_{\mathbf{k}}(t)$. As a first approach, which can be refined within the same formalism,[9,11,12,23] the electron-electron interaction $\dot{p}_{\mathbf{k}}|^{ee}$ is treated in a statically screened Hartree-Fock factorization.[20] The contributions of the electron-electron interaction take the form,

$$\dot{p}_{\mathbf{k}}|^{ee} = \frac{i}{\hbar}\sum_{\mathbf{q}} \{R^1_{(\mathbf{k},\mathbf{q})} n^c_{\mathbf{k}+\mathbf{q}} - R^2_{(\mathbf{k},\mathbf{q})} n^v_{\mathbf{k}+\mathbf{q}}\} p_{\mathbf{k}} + \frac{i}{\hbar}\sum_{\mathbf{q}} V^{vcvc}_{(\mathbf{k},\mathbf{q})} p_{\mathbf{k}+\mathbf{q}} (n^v_{\mathbf{k}} - n^c_{\mathbf{k}}). \quad (7)$$

Here, we employed the definitions $R^1_{(\mathbf{k},\mathbf{q})}=V^{cccc}_{(\mathbf{k},\mathbf{q})}-V^{cvvc}_{(\mathbf{k},\mathbf{q})}$ and $R^2_{(\mathbf{k},\mathbf{q})}=V^{vvvv}_{(\mathbf{k},\mathbf{q})}-V^{vccv}_{(\mathbf{k},\mathbf{q})}$. The screened Hartree-Fock contribution to the CNT EOM [Eq. (7)] contains an exchange shift (first sum) and an excitonic contribution (second sum), both screened; all other contributions vanish in RWA. These two contributions correspond to the self-energy and the direct contribution in a Bethe-Salpeter equation approach.[24] The first term in Eq. (7) causes a renormalization of the single-particle energies (exchange shift); the formation of excitons is due to the second term (excitonic contribution).

In the case of linear absorption [sufficiently weak incoming pulse $\mathbf{A}_0(t)$], the ground state electron occupation remains unchanged ($n^c_{\mathbf{k}}=0$ and $n^v_{\mathbf{k}}=1$). For strong optical pulses, the electron occupations $n^\lambda_{\mathbf{k}}$ have to be considered dynamically. A similar evaluation [see Eqs. (6) and (7)] gives the occupation dynamics $\dot{n}^\lambda_{\mathbf{k}}=\dot{n}^\lambda_{\mathbf{k}}|^f+\dot{n}^\lambda_{\mathbf{k}}|^{ee}$,

$$\dot{n}^v_{\mathbf{k}}|^f = \dot{n}^c_{\mathbf{k}}|^f = -2\,\text{Re}\{\Omega p_{\mathbf{k}}\},$$

$$\dot{n}^v_{\mathbf{k}}|^{ee} = -\dot{n}^c_{\mathbf{k}}|^{ee} = \frac{2}{\hbar}\,\text{Im}\left\{p^*_{\mathbf{k}}\sum_{\mathbf{q}} V^{vcvc}_{(\mathbf{k},\mathbf{q})} p_{\mathbf{k}+\mathbf{q}}\right\}. \quad (8)$$

In the following, we demonstrate the ability of the CNBEs [Eqs. (6)–(8)] to reproduce the well-known excitonic spectra.[2,6,8,22,24] However, the main purpose of our model is to describe nonlinear optics and ultrafast electron dynamics.

EXCITONS IN CARBON NANOTUBES

To benchmark the CNBEs [Eqs. (6) and (7)] and to illustrate that the Bloch equation approach reproduces well-known aspects of CNT excitons, we discuss the linear absorption of the semiconducting (11,6) CNT. We solve Eqs. (6) and (7) numerically to calculate the linear absorption spectrum (calculations were performed with a phenomenological dephasing $\gamma=12.5$ meV). The current density [Eq. (5)] can be used to calculate the absorption coefficient $\alpha(\omega)\sim\text{Im}[j_\parallel(\omega)/A_\parallel(\omega)]$ for light polarized parallel ($\parallel$) to the nanotube axis.[19] We reproduce exchange and excitonic energy shifts resulting from Eq. (7). Both contributions to the binding energy are shown in Fig. 1. The free carrier van Hove singularity, typical for a one-dimensional free tight-binding spectrum (short-dashed line), is shifted by the exchange contribution to higher energies (renormalized band edge, long-dashed line). The excitonic contribution causes a strong excitonic resonance well below the renormalized band edge (all contributions, solid line). As a result, we observe a net blueshift of the electron-electron interaction induced

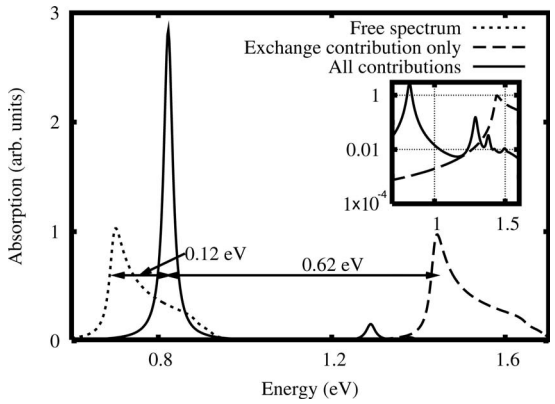

FIG. 1. Absorption spectra of the (11,6) chiral nanotube: free tight-binding calculation (short-dashed line with a resonance at 0.7 eV), HF spectra with (solid line) and without (long-dashed line, exchange shift only) excitonic contribution. The excitonic resonance at 0.82 eV [experimental value for an air suspended (11,6) nanotube (Ref. 22): 0.9 eV] lies 0.62 eV below the renormalized band edge at 1.44 eV. The inset shows details of the higher excitonic levels near the renormalized band edge.

excitonic resonance compared to the free spectrum. The inset shows the details of the excitonic spectrum near the renormalized band edge. In this logarithmic plot, higher excitonic states are visible.

The effect of an external dielectric screening ε_r caused by the surrounding material (opposed to the internal screening described by the Lindhard formula) can also be addressed [see Eq. (4)]. Here, ε_r leads to an overall suppression of the electron-electron interaction $\dot{p}_{\mathbf{k}}|^{ee}$. Hence, the excitonic resonance is redshifted toward the free band gap, and in the limit $\varepsilon_r \to \infty$, the free spectrum is obtained (not shown).

CARBON NANOTUBE GAIN SPECTRA

Next, we illustrate that the CNBEs predict exciton saturation and optical gain if electrons and holes are injected within a quasiequilibrium situation into the conduction and valence band of the CNT. $n_{\mathbf{k}}^c$ and $n_{\mathbf{k}}^v$ form Fermi-Dirac distributions $f_{\mathbf{k}}^c(N_e,T)$ and $f_{\mathbf{k}}^v(N_e,T)$, fixed by temperature T and the occupation percentage of excited electrons N_e. Here, $N_e = n^c/N_m$, where N_m is the electron density of the fully occupied valence band. Such a quasiequilibrium situation may be generated similar to semiconductor gain materials, since the relaxation times for interband transitions (radiative decay) are long in comparison to the intraband relaxation times.[25] Figure 2 shows linear absorption spectra of the (11,6) CNT for different occupations N_e ($T=77$ K). For increasing carrier density, the interplay of excitonic effects, exchange shift, and dielectric screening [Eq. (7)] leads to exciton saturation and optical gain. The broad shoulder appearing above the resonance with increasing carrier density is a signature of the free particle spectrum (see Fig. 1), which is reproduced for high carrier density. A detailed analysis of the different contributions shows that the overall redshift mainly originates from internal screening. This effect results basically from the static screening model and is probably reduced by dynamical

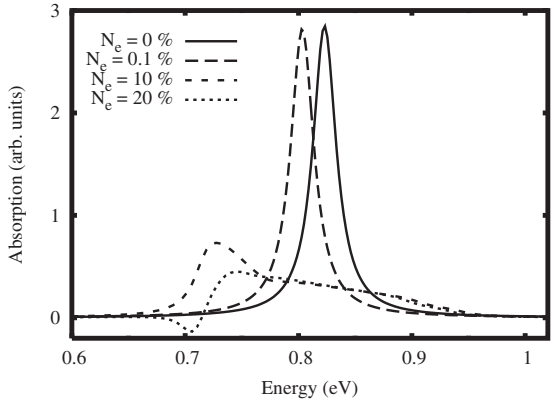

FIG. 2. Absorption spectra of the (11,6) nanotube for different occupation densities N_e at $T=77$ K. A finite occupation density yields a redshift and bleaching of the excitonic resonance. At high occupations, the absorption changes into gain as a result of occupation inversion.

screening.[26] At about $N_e=20\%$, optical gain (negative absorption) occurs, since the occupation at $\mathbf{k}$ states near the band minimum is inverted. Such gain calculations are a prerequisite for future CNT lasers.

ADIABATIC FOLLOWING AND RABI OSCILLATIONS

In order to demonstrate the ability of the CNBEs to describe the many-body response to ultrafast pulses, we discuss two effects known from two level systems: adiabatic following and Rabi oscillations.[23,27] Here, we focus on off-resonant (detuning Δ below linear excitonic resonance) excitation where electron-electron scattering is not important and the Hartree-Fock approximation is a valid description. Figure 3 shows the dynamics of the electron occupation $N_e = n^c(t)/N_m$ [see Eq. (5)] if a CNT is excited by a 118 fs (full width at half maximum) pulse. For detuning Δ of 100 meV (or larger), the occupation density adiabatically follows the

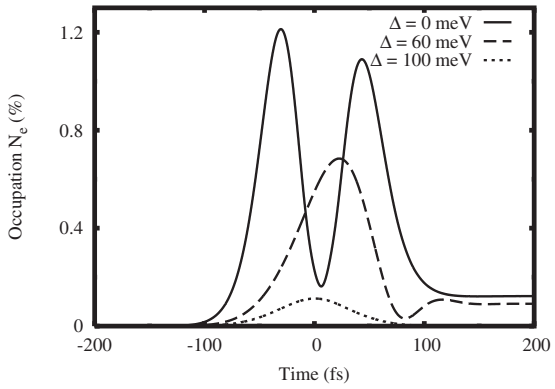

FIG. 3. Occupation dynamics of the (11,6) CNT with $\hbar\Omega_m = 21$ meV and $\sigma=50$ fs for different detunings Δ. For off-resonant excitation ($\Delta=100$ meV), it is seen that the occupation density follows the pump pulse (adiabatic following). With decreasing detuning Δ, the occupation increases. At about $\Delta=60$ meV, Rabi oscillations begin, which are even more pronounced at $\Delta=0$ meV.

pump pulse.[23] With decreasing detuning Δ, the excited carrier density is increased; below $\Delta=60$ meV, density oscillations between the conduction and valence band (*Rabi flopping*) set in.

DYNAMICAL STARK EFFECT

In experiments, the detection of pump-induced electron dynamics $n^{\lambda}(t)$ can be studied using a pump-probe setup. After a delay time τ, the pump-induced response of the system is probed by an ultrashort resonant probe pulse. To assure the validity of the Hartree-Fock approximation, we focus on the off-resonant pump excitation (see Fig. 3) for $\Delta=100$ meV. Hence, the off-resonant pump pulse excites only virtual occupations to the conduction band near the band minimum that follow adiabatically (see Fig. 3). Additionally, to suppress relaxation contributions beyond the Hartree-Fock approximation, the calculations are performed for $\tau=0$.[28] First, the density dynamics induced by the pump pulse (without the probe pulse) are calculated. As the weak and short probe pulse does not affect the excited carriers, the pump pulse induced dynamics can be used to obtain a probe spectrum. Figure 4 shows the absorption spectra for different maximum amplitudes $A_{\parallel}^{m}$ of the pump pulse given in terms of the maximum Rabi frequency $\Omega_m=e_0A_{\parallel}^{m}\max(M_{\parallel\mathbf{k}}^{vc})/m_0$. Due to the virtual electron density excitation in the conduction band, the excitonic resonance is shifted due to the Coulomb-induced energy and field renormalization and the internal screening [Eq. (7)].

CONCLUSION

Many-body optical Bloch equations for carbon nanotubes (CNBEs) offer the potential to go beyond linear optics and to describe the nonlinear electron dynamics in optically excited CNTs. In the present version of the CNBEs, the electron-electron interaction is included within a screened Hartree-Fock approximation. To improve the theory, higher Coulomb correlations such as electron-electron scattering or multiexciton states as well as electron-phonon (polaron) interaction can be included in a self-consistent way similar to Refs. 9–12, 23, and 29 for semiconductors. Next, improvements should address (non-Markovian) self-energy shifts and electron-electron scattering induced by correlation effects to check the validity range of the screened Hartree-Fock approach. We hope that our work stimulates more research in nonlinear and ultrafast[30] phenomena in CNTs.

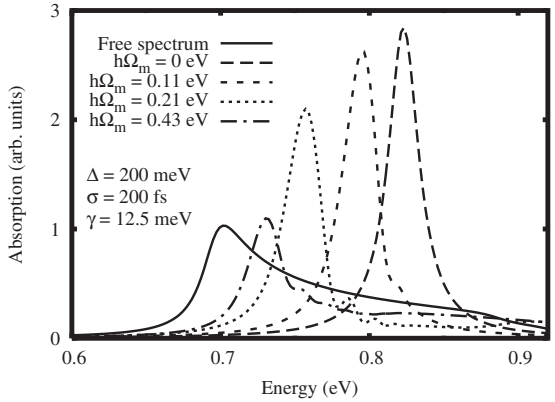

FIG. 4. Pump-probe spectra ($\Delta=200$ meV, $\sigma=200$ fs) of a (11,6) CNT for different vector potential amplitudes A (dashed lines) given in terms of the maximum Rabi frequency Ω_m of the pulse and free linear absorption spectrum (solid line). For increasing amplitude, the spectrum approaches the linear spectrum (redshift and bleaching). The humps in the spectra for $\Omega_m\neq 0$ stem from higher excitonic levels that are shifted toward the main resonance as the increased screening reduces the excitonic binding energy.

ACKNOWLEDGMENTS

Support from the Cluster of Excellence "Unifying Concepts in Catalysis" (DFG) is acknowledged. We thank Studienstiftung des Deutschen Volkes and DFG for financial support.

*matthias@itp.physik.tu-berlin.de

[1] F. Wang, G. Dukovic, L. Brus, and T. Heinz, Science **308**, 838 (2005).
[2] J. Maultzsch, R. Pomraenke, S. Reich, E. Chang, D. Prezzi, A. Ruini, E. Molinari, M. S. Strano, C. Thomsen, and C. Lienau, Phys. Rev. B **72**, 241402(R) (2005).
[3] V. Perebeinos, J. Tersoff, and P. Avouris, Phys. Rev. Lett. **94**, 027402 (2005).
[4] J. Ma and R. K. Yuan, Phys. Rev. B **57**, 9343 (1998).
[5] M. P. Lopez Sancho, M. C. Muñoz, and L. Chico, Phys. Rev. B **63**, 165419 (2001).
[6] C. D. Spataru, S. Ismail-Beigi, L. X. Benedict, and S. G. Louie, Phys. Rev. Lett. **92**, 077402 (2004).
[7] V. Perebeinos, J. Tersoff, and P. Avouris, Phys. Rev. Lett. **92**, 257402 (2004).
[8] E. Chang, G. Bussi, A. Ruini, and E. Molinari, Phys. Rev. Lett. **92**, 196401 (2004).
[9] M. Lindberg and S. W. Koch, Phys. Rev. B **38**, 3342 (1988).
[10] F. Rossi and T. Kuhn, Rev. Mod. Phys. **74**, 895 (2002).
[11] I. Waldmüller, J. Förstner, S.-C. Lee, A. Knorr, M. Woerner, K. Reimann, R. A. Kaindl, T. Elsaesser, R. Hey, and K. H. Ploog, Phys. Rev. B **69**, 205307 (2004).
[12] I. Waldmueller, W. W. Chow, and A. Knorr, Phys. Rev. B **73**, 035433 (2006).
[13] R. Saito, G. Dresselhaus, and M. Dresselhaus, *Physical Properties of Carbon Nanotubes* (World Scientific, Singapore, 2003).
[14] S. Reich, C. Thomsen, J. Maultzsch, and M. Janina, *Carbon Nanotubes: Basic Concepts and Physical Properties* (Wiley-VCH, New York, 2004).
[15] Y. Z. Ma, L. Valkunas, S. L. Dexheimer, S. M. Bachilo, and G. R. Fleming, Phys. Rev. Lett. **94**, 157402 (2005).
[16] G. N. Ostojic, S. Zaric, J. Kono, V. C. Moore, R. H. Hauge, and

R. E. Smalley, Phys. Rev. Lett. **94**, 097401 (2005).
[17] A. Grüneis, R. Saito, G. G. Samsonidze, T. Kimura, M. A. Pimenta, A. Jorio, A. G. Souza Filho, G. Dresselhaus, and M. S. Dresselhaus, Phys. Rev. B **67**, 165402 (2003).
[18] S. V. Goupalov, Phys. Rev. B **72**, 195403 (2005).
[19] E. Malić, M. Hirtschulz, F. Milde, A. Knorr, and S. Reich, Phys. Rev. B **74**, 195431 (2006).
[20] H. Haug and S. W. Koch, *Quantum Theory of the Optical and Electronic Properties of Semiconductors* (World Scientific, Singapore, 2004).
[21] T. Ando, J. Phys. Soc. Jpn. **66**, 1066 (1997).
[22] Y. Ohno, S. Iwasaki, Y. Murakami, S. Kishimoto, S. Maruyama, and T. Mizutani, Phys. Rev. B **73**, 235427 (2006).
[23] R. Binder, S. W. Koch, M. Lindberg, N. Peyghambarian, and W. Schäfer, Phys. Rev. Lett. **65**, 899 (1990).
[24] J. Jiang, R. Saito, G. G. Samsonidze, A. Jorio, S. G. Chou, G. Dresselhaus, and M. S. Dresselhaus, Phys. Rev. B **75**, 035407 (2007).
[25] Modifications of the electron distributions and relaxation dynamics due to dark excitonic states, which can present an important relaxation channel, will be investigated in future research.
[26] S. Das Sarma and D. W. Wang, Phys. Rev. Lett. **84**, 2010 (2000).
[27] L. Allen and J. Eberly, *Optical Resonance and Two Level Atoms* (Dover, New York, 1987).
[28] For instance, the phonon scattering of optically active electrons into the dark excitonic state below the dipole allowed resonance induces decay times of several hundreds of femtoseconds (Ref. 31) too long to affect the occupation dynamics dramatically.
[29] S. Butscher and A. Knorr, Phys. Rev. Lett. **97**, 197401 (2006).
[30] A. Rozhin, Y. Sakakibara, H. Kataura, S. Matsuzaki, K. Ishida, Y. Achiba, and M. Tokumoto, Chem. Phys. Lett. **405**, 288 (2005).
[31] Y. Z. Ma, C. D. Spataru, L. Valkunas, S. G. Louie, and G. R. Fleming, Phys. Rev. B **74**, 085402 (2006).